Acta Universitatis Sapientiae
Electrical and Mechanical Engineering, 2 (2010) 146-158

Microstructural Modification of $(Ti_{1-x}Al_xSi_y)N$ Thin Film Coatings as a Function of Nitrogen Concentration

Domokos BIRÓ [1], Sándor PAPP [2], László JAKAB-FARKAS [2]

[1] Department of Mechanical Engineering, Faculty of Technical and Human Sciences, Sapientia University, Tg. Mureş, e-mail: dbiro@ms.sapientia.ro
[2] Department of Electrical Engineering, Faculty of Technical and Human Sciences, Sapientia University, Tg. Mureş, e-mail: spapp@ms.sapientia.ro, jflaci@ms.sapientia.ro

Manuscript received November 02, 2010; revised November 24, 2010.

Abstract: In the past few years a considerable research activity has been directed towards understanding the structure forming phenomena of nanostructured materials. A wide range of composition and structure of multiphase material systems have been investigated in order to allow a fine tuning of their functional properties. We have studied one of the most promising material systems composed of Al, Ti, Si, N, where a significant reduction in grain growth was achieved through control of phase separation process. Nanostructured (Al, Ti, Si)N thin film coatings were synthesized on Si(100) and high speed steel substrates by DC reactive magnetron sputtering of a planar rectangular Al:Ti:Si=50:25:25 alloyed target, performed in Ar/N_2 gas mixture. For all the samples we have started with deposition of a nitrogen-free TiAlSi seed layer. Cross-sectional transmission electron microscopy investigation (XTEM) of as-deposited films revealed distinct microstructure evolution for different samples. The metallic AlTiSi film exhibited strong columnar growth with a textured crystalline structure. Addition of a small amount of nitrogen to the Ar process gas caused grain refinement. Further increase of nitrogen concentration resulted in fine lamellar growth morphology consisting of very fine grains in close crystallographic orientation showing up clusters of the chain-like pearls in a dendrite form evolution. Even higher N concentration produced homogeneous compact coating, with an isotropic structure in which we can observe nanocrystals with average size of ~3nm. The kinetics of structural transformations is explained in the paper by considering the basic mechanism of spinodal decomposition process.

Keywords: Nanostructured (Ti,Al,Si)N thin films, cross-sectional transmission electron microscopy (XTEM) investigation, grain refinement, lamellar growth morphology, spinodal decomposition.

1. Introduction

In the last decade intense research activity was devoted to investigate nanocomposite coating materials, consisting of a nanocrystalline transition metal nitride and an amorphous tissue phase. These coating materials are characterized by high hardness [1], enhanced elasticity [2] and high thermal stability [3], which define their unusual mechanical and tribological properties. Various studies revealed that in multiphase nanocomposite materials the microstructure and the ratio between hardness and elastic modulus H/E are important in the coating performance [4]. Recently the most studied material is the quaternary (Ti, Al, Si)N nitride system revealing the most promising results.

As it has been suggested by *Veprek* [5], in nanocomposite materials the structure and size of the nanocrystalline grains embedded in the amorphous tissue phase together with the high cohesive strength of their interface, are the main parameters which control the mechanical behavior of the coatings. The reported results revealed that adatom mobility may control the microstructure evolution in multi-elemental coating systems, where the substrate temperature and the low energy ion/atom arrival ratio have significant effect on the growth of nanocrystalline grains.

The microstructure and growth mechanism of arc plasma deposited TiAlSiN (35 at.% Ti, 42 at.% Al, 6.5at.% Si) thin films were investigated by *Parlinska et al.* [6, 7]. It was shown that compositionally graded TiAlSiN thin films with Ti-rich zone close to the substrate exhibited crystalline structure with pronounced columnar growth. Addition of Al+Si leads to a grain refinement of the coatings, and a further increase of the Al+Si concentration results in the formation of nanocomposites, consisting of equiaxial, crystalline nanograins surrounded by a disordered, amorphous SiN_x phase.

In our study (Al, Ti, Si)N single layer thin film coatings were deposited on Si(100) and high-speed steel substrates by DC reactive magnetron sputtering. We investigated the micro structural modification of $(Ti_{1-x}Al_xSi_y)N$ thin film coatings as a function of nitrogen concentration by conventional transmission electron microscopy.

2. Experimental details and characterization technique

Deposition experiments of (Al, Ti, Si)N quaternary nitride coatings were carried out in a laboratory scale equipment by DC driven magnetron sputtering, whose details are reported elsewhere [8]. The three independently operated sputter sources were closely arranged side by side on the neighboring vertical walls of a 75 *l* octagonal all-metal high vacuum chamber. The closely disposed UM magnetrons arranged on an arc segment were highly interacting by their

magnetic fields, leading to a far extended active plasma volume. In the presented deposition experiments only the central magnetron source was active, while the adjacent two magnetron sources contributed only in the closed magnetic field. A high purity planar rectangular target material of alloyed AlTiSi was used. Elemental composition of the PLANSEE GmbH. alloyed target was 50 at.% Al, 25 at.% Ti, and 25 at.% Si, with 165×85×12 mm^3 in size, which was partially covered on the erosion zone with a high purity 99.98% Ti sheet. Prior to deposition in the vacuum chamber a base pressure of $2 \cdot 10^{-4}$ Pa was established by operating a 540 l/s turbo molecular pump.

Polycrystalline high-speed steel (HSS) substrates were used for tribological measurements, and native SiO_2 covered mono-crystalline <100> Si wafers were also used as substrates for XTEM microstructure investigation of the as-deposited (Al, Ti, Si)N single layer thin film coatings. The target-to-substrate distance was kept constant at 110 mm in all runs. The substrates were positioned in static mode on a molybdenum sheet substrate holder, which allowed application of $U_s = -75$ V bias voltage. The Mo sheet was externally heated to a controllable substrate temperature of $T_s = 400$ ºC.

Prior to the starting of the deposition process, the surface of the substrates was plasma-etched by a DC glow discharge in argon for 10 min at 0.8 Pa, while the bias voltage was limited up to 350 V. During the ion etching of substrates, the target surfaces were also sputter cleaned by operating the magnetron unit at limited discharge power (pre-sputtering power of 150 W). The substrate surfaces were shielded during the pre-sputtering. The reactive sputtering process was performed in a mixture of Ar and N_2 atmosphere at 0.28 Pa pressure. During the reactive sputtering process the nitrogen mass flow rate was controlled with an Aalborg DFC 26 flow controller, which contains a solenoid valve. The argon gas throughput ($q_{Ar} = 6.0$ sccm, measured by GFM 17 Aalborg mass flow meter) was adjusted by a servo motor driven mass flow rate controller (MFC-Granville Phillips S 216).

A constant sputtering power with a current density of 10 $mA \cdot cm^{-2}$ was selected for about 10 min sputter cleaning of the targets. During deposition the discharge power at the target surface was raised to 500 W, and the development of coating started with the deposition of a 50 nm thick AlTiSi metallic seed-layer performed in pure Ar atmosphere. In the next step of deposition an (Al, Ti, Si)(N) interlayer with gradient composition was reactively grown, while PC controlled N2 flow rate was increased slowly up to the pre-selected value. The argon gas flow was kept constant at 6.0 sccm. The typical thickness of the coatings was approximately 2 μm.

The experimental conditions for preparation of (Al, Ti, Si)N coatings are listed in *Table 1*. The microstructure and growth morphology of the as-deposited coatings was examined by use of a 100 kV operated JEOL 100U

transmission electron microscope. In order to prepare cross-sectional XTEM samples for transverse observations, the samples were subjected to ion-milling in view of thinning up to electron beam transparency. Thin specimens for XTEM investigations were prepared in a Technoorg-Linda Ltd. model 4IV/H/L ion beam thinning unit. High energy ion beam thinning was completed with a low angle and low energy (200 eV) ion beam process in order to eliminate the amorphous by-products and etching defects induced by the high energy ions.

Table 1: Summary of deposition parameters used for preparation of (Al, Ti, Si)N coatings: P_d- DC magnetron discharge power, q_{N2}- nitrogen mass flow rate, T_s- substrate temperature, U_s- substrate bias voltage.

Samples	P_d [W]	q_{N2} [sccm]	T_s [°C]	U_s [V]
TiS_01	500	-	400	-75
TiS_07	500	1.0	400	-75
TiS_08	500	1.0	400	-75
TiS_04	500	2.0	400	-75
TiS_09	500	2.0	400	-75
TiS_10	500	2.0	100	-75
TiS-06	500	3.0	400	-75
TiS-03	500	4.0	400	-75
TiS-05	500	5.0	400	-75
TiS-02	500	6.0	400	-75

Bright-field (BF) and dark-field (DF) transmission imaging techniques were used for microstructure investigation of the as-prepared samples. The identification of the crystallographic phases and the crystal orientation were also performed by evaluation of selected area electron diffraction (SAED) patterns. The SAED patterns were processed with the ´Process-Diffraction´ software tool developed by *Labar* [9].

3. Results and discussion

In this XTEM study of our prepared (Al, Ti, Si)N coatings, we combined direct imaging and selected area electron diffraction modes (SAED), which

facilitate obtaining information on the microstructure morphology, grain size and crystallographic preferred orientation.

Cross-sectional image of the metallic polycrystalline AlTiSi coating's columnar structured morphology is given in *Fig. 1*. The micrograph shows that the crystallite in a conical shape evolution starts close to the substrate and grows in a competitive mode. The columns with crystalline grains grow through the entire film thickness up to the top surface of the coating. The columnar grains are normally oriented to the substrate's surface. The large AlTi(Si) crystallites of approximately 80 nm in width are separated by the more electron-transparent $TiSi_2$ phase segregated to the grain boundaries. The SAED patterns taken from the bulk region of the film exhibit well-defined spotted diffraction rings (not to be seen here). The SAED pattern taken from the near substrate region of the coating proved crystalline character of the Si doped TiAl film (inset of *Fig. 1.*). The phases that can be derived from the diffraction pattern are mainly fcc-B1 NaCl-type of TiAlSi solid solution crystallites. The simulation of the diffraction rings was performed taking into account an fcc-type structure. It can be clearly seen the <200> preferential growth direction, indicated by significant brightness increase due to reflections from (200) crystallite planes that are oriented in parallel to the growing surface.

The chemical composition of the as deposited TiAlSi thin film was evaluated from EDS spectra analysis, and found to be of 34 at.% Ti, 46 at.% Al and 20 at.% Si.

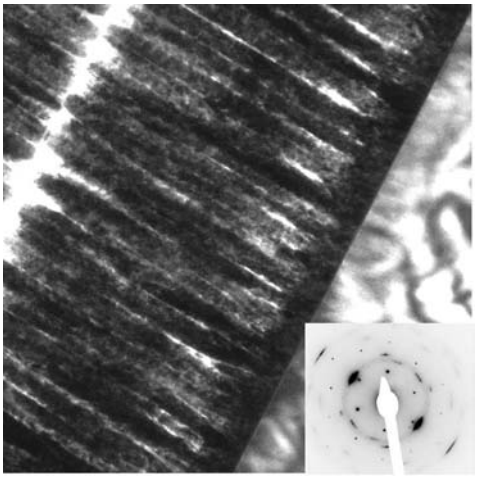

Figure 1: XTEM micrograph showing a cross-sectional view of the columnar structured polycrystalline TiAlSi thin film coating (TiS_01 sample). The inset of SAED electron diffraction pattern indicates an fcc-structured TiAlSi solid solution phase, showing (200) texture evolution in the growing direction.

By adding a small amount of nitrogen as reactive gas in the argon process gas, the growth morphology of the film dramatically changed (*Fig. 2*).

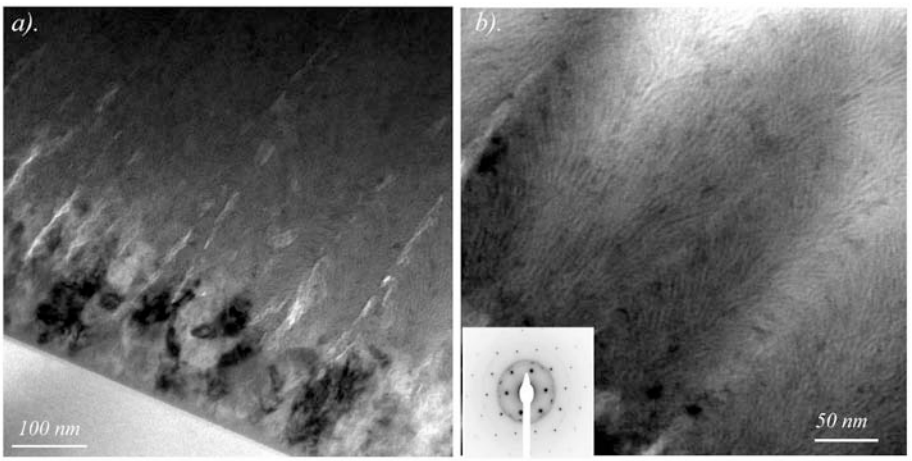

Figure 2: XTEM micrograph and SAED electron diffraction pattern of the (AlTiSi)N coating grown by nitrogen flow rate of q_{N2}=2 sccm (sample TiS_09): a). Bright field (BF) image indicates a weakly columnar structure evolution in close vicinity of transition zone from the ternary TiAlSi sub-layer to the quaternary (AlTiSi)N overgrown layer, b). On the enlarged micrograph slightly curved fine lamellar growth morphology could be identified inside the individual columns.

For a nitrogen flow rate of q_{N2} = 2 sccm the microstructure indicates a weak columnar evolution (*Fig. 2a*). Slightly curved fine lamellar growth morphology could be identified inside of the individual columns (see on the enlarged micrograph, *Fig. 2b*).

Selected area electron diffraction pattern (SAED) performed in close vicinity of transition zone –including also the Si(100) bulk–, claims for a two-phase mixture of fcc-TiAlN nanocrystals embedded in an amorphous tissue phase (inset of *Fig. 2b*). Furthermore, (200) preferential growth in close vicinity of transition zone from the ternary TiAlSi sub-layer to the quaternary (AlTiSi)N overgrown layer was slightly maintained. The presence of continuous reflection rings suggests a grain refinement of the coating with a strong tendency for evolution from the textured polycrystalline phase to a mixture of nanocrystalline AlTi(Si)N phase and possible formation of silicon nitride amorphous tissue phase.

Chemical composition of the as deposited (Ti, Al, Si)N thin films was evaluated from EDS spectra, and found to be 23 at.% Ti, 46 at.% Al, 26 at.%. Si, and about 5 at.% N.

With further increase of nitrogen amount in the coating deposition process (TiS_05 sample performed by q_{N2} =5 sccm nitrogen flow rate, which determined in our reactive magnetron sputtering process a p_N = 0.0016 mbar nitrogen partial pressure) the crystalline character of the coating disappeared and formed an isotropic nanocomposite structure, possibly consisting of nanocrystalline $Ti_3AlN/TiSi_2$ grains of 2…3 nm in size surrounded by Si_xN_y and/or AlN amorphous matrix phase (*Fig. 3a*). The SAED diffraction pattern revealed that an increased nitrogen amount leads to a nanocomposite structure, consisting of equiaxially distributed $Ti_3AlN/TiSi_2$ nanocrystalline grains surrounded by a very thin amorphous Si_3N_4 phase.

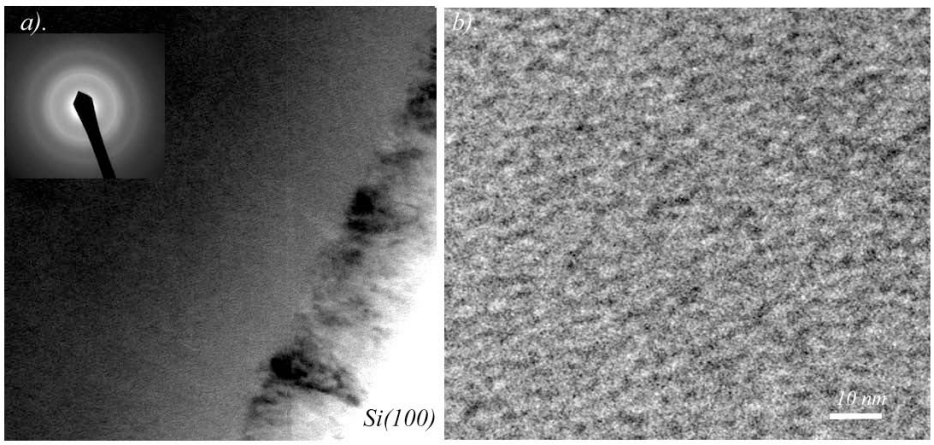

Figure 3: Bright field XTEM micrograph of (AlTiSi)N thin film deposited with an increased nitrogen flow rate (TiS_05 sample, q_{N2}=5 sccm): a). The coating's microstructure indicates the development of a competitive columnar evolution of the ternary TiAlSi sub-layer followed by the growth of the quaternary (AlTiSi)N overgrown layer developed in an isotropic morphology. b). The enlarged micrograph clearly shows a random distribution of very fine *nc*-($Al_{1-x}Ti_x$)N grains, having an average size of ~ 3 nm, with disordered grain limiting boundaries.

The chemical composition of the as deposited thin film was evaluated from EDS spectra analysis, and found to be 12 at.% Ti, 19 at.% Al, 23 at.% Si and 46 at.% N. The oxygen impurity content decreased to about 0.2 % which was related to a prolonged outgassing process of the vacuum chamber and thermal degassing of the substrate by heating to 600 °C prior to the deposition process.

Veprek et. al [10, 11] in their recently published review paper emphasized that ultra-hard nanocomposite nitride phase coatings based on (Ti, Al, Si)N elemental composition can be managed by well-controlled plasma and deposition conditions. The development in a periodic structure of the

nc-($Al_{1-x}Ti_x$)N/*a*-Si_3N_4 nanocomposite coatings, composed from the uniformly distributed ($Al_{1-x}Ti_x$)N nanocrystals and amorphous tissue phase of Si_3N_4 with about one monolayer (ML) thickness, was explained by the spontaneous separation in spinodal decomposition and self-organization upon phase segregation process. The strong immiscibility of Si_3N_4 phase in crystalline TiAlN phase, as well the absence of the Ostwald ripening, are appropriate conditions for the development of nanocomposite coatings.

Favvas and *Mitropoulos* [12] in their paper (see also the cited paper therein) compiled the IUPAC definition of spinodal decomposition: "A clustering reaction in a homogeneous, supersaturated solution (solid or liquid) which is unstable against infinitesimal fluctuations in density or composition. Therefore, homogeneous solution separates spontaneously into two phases, starting with small fluctuation and proceeding with decrease in the Gibbs free energy without a nucleation barrier. "

It is known from thermodynamic theory that by fast cooling of a homogeneous solution the diffusion process occurs with net reduction in Gibbs free energy of the system. The free energy of mixing, ΔG^{mix}, defined by the thermodynamic equation of Gibbs has a general form:

$$\Delta G^{mix} = \Delta H^{mix} - T \cdot \Delta S^{mix}, \tag{1}$$

where the enthalpy change ΔH^{mix} is associated with the interactions between the components of the mixture, and the entropy change ΔS^{mix} is associated with the random mixing of components.

At high temperature of the system, with partially miscible components *A* and *B*, the components give rise to a continuous solution (in a liquid or solid phase) due to a complete solubility. At lower temperature the solution becomes unstable and may exists compositional ranges where the co-existing solid phases are more stable.

Therefore, during the cooling of liquid, phase separation proceeds in order to minimize the free energy. If the super-cooling of the homogeneous solution takes place into the coherent spinodal region, defined by the compositional interval between points of inflexion on the free energy diagram as a function of molar composition $G = f(X_A)$, the phase separation process occurs by the decomposition of the homogeneous solution. Decomposition is favored by small fluctuations produced in the chemical composition or infinitesimal perturbations in chemical potential. In accordance with Fick's first law, the diffusion flux of a component, e.g. j_A is proportional to the concentration gradient of the respective component *A*, $\frac{\partial C_A}{\partial x}$:

$$j_A = -D_A \cdot \frac{\partial C_A}{\partial x}, \tag{2}$$

where D_A stands for diffusion coefficient in the first empirical law of Fick.

The diffusion flux j_A can be driven also by the free energy gradient of component *A*:

$$j_A = -C_A \cdot \mu_A \cdot \frac{\partial G_A}{\partial x}, \tag{3}$$

where μ_A stand for the mobility constant of component *A*.

From the above equations the diffusion coefficient D_A can be written as a derivative function of the Gibbs free energy in respect to the concentration:

$$D_A = C_A \cdot \mu_A \cdot \frac{\partial G_A}{\partial C_A} \tag{4}$$

If the diffusion coefficient is positive, $D_A > 0$, i.e. $\frac{\partial G_A}{\partial C_A} > 0$, the chemical potential gradient has the same direction as the concentration gradient, therefore the diffusion flux occurs along the concentration gradient. For diffusion coefficient $D_A < 0$, i.e. $\frac{\partial G_A}{\partial C_A} < 0$, the diffusion flux occurs against to the concentration gradient.

By correlating the phase composition diagram (i.e. a diagram of phases, where the dependence for temperature *T* versus the molar fractions X_A and X_B of components indicates the composition ranges for equilibrium phases) and the diagram of the free energy change versus the molar fraction of the mixture, it can be seen that below the spinodal (where the second derivative of the free energy of mixing versus the molar fraction X_A is zero, $\frac{\partial^2 \Delta G}{\partial X_A^2} = 0$) the system is unstable (*Fig. 4*).

For negative values of the second derivative of the free energy of mixing versus the molar fraction X_A, e.g. of component *A*, i.e. $\frac{\partial^2 \Delta G}{\partial X_A^2} < 0$, the homogeneous supersaturated solution is unstable and spinodal decomposition may proceed.

The spinodal decomposition process happens in an unstable region, where further instability is caused by the small fluctuation occurred in the local concentration, while the diffusion process takes place from the lower to higher concentration (i.e. “up-hill” diffusion).

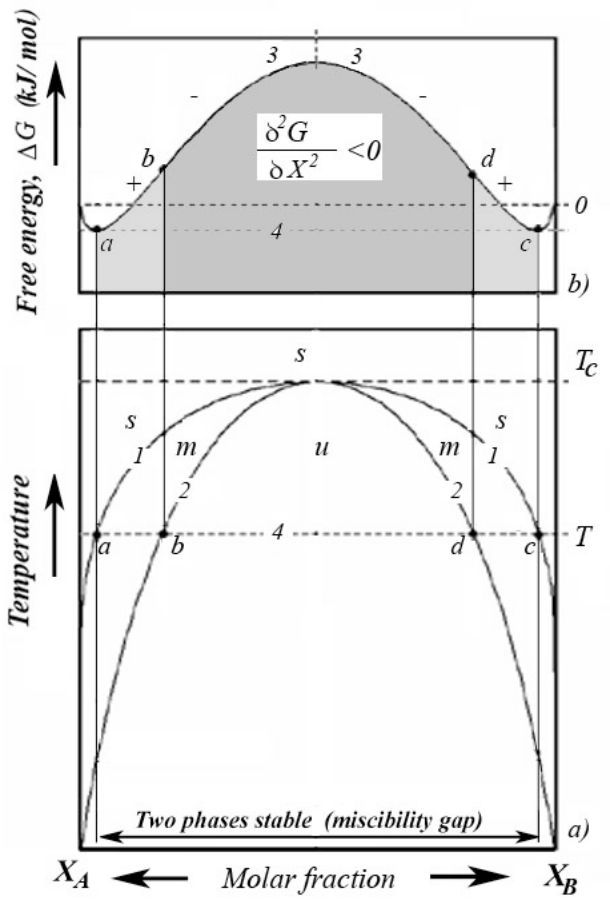

Figure 4: Illustration of the spinodal decomposition on the phase separation mechanism: *a*). Equilibrium phase diagram with the phase boundary limits: for a temperature *T* of the system points *a* and *c* stand for compositional interval of miscibility gap (with two stable solid phases), the interval between points *b* and *d* stand for the spinodal limits; *b*). Diagram of the Gibbs free energy changes in the mixing process of two partially miscible components *A* and *B*, boundary line (1) separates a stable region (*s*) of the homogeneous liquid phase and the metastable region (*m*) of the precipitated solid phases. Line (2) is the limit of spinodal, below of which the thermodynamically unstable system (*u*) turns from one phase (liquid) to a mixture of two phases (solid) system with different elemental composition

Therefore, spinodal decomposition process is a spontaneous reaction, which is the main route to develop periodic structures with uniform size.

Our experimental results on fine lamellar growth morphology of (Ti, Al, Si)N nitride coatings, consisting of chain-like pearls in a dendrite evolution with very fine grains in close crystallographic orientation, may be explained in accordance with Veprek's theory by partial spinodal decomposition and phase segregation during the film's growth while percolation threshold composition is attained by an increased nitrogen activity.

On the other hand, the increase of deposition rate induces a decrease of the surface mobility related to the decrease of the ion-to-atom arrival rate ratio. These particular deposition conditions explain the columnar structure of TiAlSi solid solution crystallites, which can be clearly observed in the XTEM image of TiS_01 sample. Addition of minor amounts of nitrogen leads to an encapsulation of the growing TiAl(Si)N crystallites by process segregated amorphous phase.

From the detailed observation of the SAED diffuse diffraction pattern of sample TiS_05 obtained with an increased nitrogen flow rate, the presence of an amorphous phase surrounding the Ti_3AlN nanocrystallites can be attributed to Si_3N_4 matrix phase (inset of *Fig. 3a*). The formation of amorphous $TiSi_2$ and AlN phase due to the partial segregation of Al and Si atoms should be also considered due to the effect of enhanced ion bombardment provided by the focused plasma beam that is characteristic to the present experimental conditions [8].

When the atomic surface mobility in the growing film is adequate, the segregated atoms can nucleate and develop the new phases controlled by deposition temperature and by the energy transfer from an increased incident ion-to-atom arrival rate ratio [13-15].

Further experiments are in progress to investigate the influence of the deposition temperature on structure evolution of (TiAlSi)N coatings.

4. Conclusions

In the present work it was shown that:

a) Columnar structure of polycrystalline AlTiSi thin film coating evolved by non-reactive DC magnetron sputtering applied to Al:Ti:Si = 50:25:25 alloyed target (performed in pure Ar atmosphere, where the 500 W discharge power, T_s = 400 ºC substrate temperature and U_s = –75 V bias voltage were held constants).

b) Addition of a small amount of nitrogen to the process gas leads to a grain refinement of polycrystalline (Ti, Al, Si)N thin films. Increase of N concentration (q_{N2} = 2 sccm flow rate) resulted in fine lamellar growth *m*orphology of coatings, showing chain-like pearls in a dendrite evolution, consisting of clusters of very fine grains in close crystallographic orientation.

c) Further increase in the nitrogen amount (q_{N2} = 5 sccm) leads to evolution of a nanocomposite coating consisting of crystalline Ti_3AlN nanograins in 2…3 nm size surrounded by an amorphous Si_xN_y covalent nitride and/or AlN matrix phase.

d) Kinetics of the structural transformations were explained by considering the basic mechanism of spinodal decomposition process.

Acknowledgements

The authors are thankful for the financial support of this project granted by Sapientia Foundation – Institute for Scientific Research, Sapientia University. The EDS analyses of the investigated coatings were performed in a CM 20 Philips 200kV TEM electron microscope by Professor P. B. Barna from RITPMS, Budapest. Professor P. B. Barna's contribution to investigating elemental composition and the valuable discussions are highly appreciated.

References

[1] Yoon, J. S., Lee, H. Y., Han, J., Yang, S. H., Musil, J., "The effect of Al composition on the microstructure and mechanical properties of WC–TiAlN superhard composite coating", *Surface and Coatings Technology*, vol. 142-144, pp. 596-602, 2001.

[2] Duran-Drouhin, O., Santana, A. E., Karimi, A., "Mechanical properties and failure modes of TiAl(Si)N single and multilayer thin films", *Surface and Coatings Technology*, vol. 163-164, pp. 260-266, 2000.

[3] Musil, J. and Hruby, H., "Superhard Nanocomposite $Ti_{1-x}Al_xN$ Films Prepared by Magnetron Sputtering" , *Thin Solid Films*, vol. 365, pp. 104-109, 2000.

[4] Ribeiro, E., Malczyk, A., Carvalho, S., Rebouta, L., Fernandes, J. V., Alves, E., Miranda, A. S., "Effect of ion bombardment on properties of d.c. sputtered superhard (Ti,Si,Al)N nanocomposite coatings", *Surface and Coatings Technology*, vol. 151-152, pp. 515-520, 2002.

[5] Veprek, S., "New development in superhard coatings: the superhard nanocrystalline-amorphous compositics", *Thin Solid Films.* vol. 317, pp. 449-454, 1998.

[6] Parlinska-Wojtan, M., Karimi, A., Cselle, T., Morstein, M., "Conventional and high resolution TEM investigation of the microstructure of compositionally graded TiAlSiN thin films", *Surface and Coatings Technology*, vol. 177-178, pp. 376-381, 2004.

[7] Parlinska-Wojtan, M., Karimi, A., Coddet, O., Cselle, T., Morstein, M., "Characterization of thermally treated TiAlSiN coatings by TEM and nanoindentation", *Surface and Coatings Technology*, vol. 188-189, pp. 344-350, 2004.

[8] Biro, D., Barna, P. B., Szekely, L., Geszti, O., Hattori, T., Devenyi, A., "Preparation of multilayered nanocrystalline thin films with composition-modulated interfaces", *Nuclear Instruments and Methods in Physics Research* vol. 590, pp. 99-106, 2008.

[9] Lábár, J. L., "ProcessDiffraction: A computer program to process electron diffraction patterns from polycrystalline or amorphous samples", *Proceedings of the XII EUREM*, Brno (L. Frank and F. Ciampor, Eds.), vol. III., pp. I 379-380, 2000.

[10] Veprek, S., Veprek-Heijman, M. G. J., Karvankova, P., Prochazka, J., "Different approaches to superhard coatings and nanocomposites", *Thin Solid Films*, vol. 476, pp. 1-29, 2005.

[11] Veprek, S., Zhang, R. F., Veprek-Heijman, M. G. J., Sheng, S. H., Argon, A. S., "Superhard nanocomposites: Origin of hardness enhancement, properties and applications", in *Surf. And Coat. Technol.*, vol. 204, pp. 1898-1096, 2009.

[12] E. P. Favvas, A. Ch. Mitropoulos: "What is spinodal decomposition?", *Journal of Engineering Science and Technology Review*, vol. 1, pp. 15-27, 2008.

[13] Carvalho, S., Rebouta, L., Ribeiro, E., Vaz, F., Dennnot, M. F., Pacaud, J., Riviere, J. P., Paumier, F., Gaboriaud, R. J., Alves, E., "Microstructure of (Ti,Si,Al)N nanocomposite coatings", *Surface and Coatings Technology*, vol. 177-178, pp. 369-375, 2004.

[14] Carvalho, S., Rebouta, L., Cavaleiro, A., Rocha, L. A., Gomes, J., Alves, E., "Microstructure and mechanical properties of nanocomposite (Ti,Si,Al)N coatings", *Thin Solid Films*, vol. 398-399 , pp. 391-396, 2001.

[15] Vaz, F., Rebouta, L., Goudeau, P., Pacaud, J., Garem, H., Riviere, J. P., Cavaleiro, A., Alves, E., "Characterization of TiSiN nanocomposite films", *Surface and Coatings Technology*, vol. 133-134 , pp. 307-313, 2000.